Suitability of Double Hybrid Density Functionals and Their Dispersion-Corrected Counterparts in Producing the Potential Energy Curves for CO_2-Rg (Rg: He, Ne, Ar and Kr) Systems

Prasenjit Seal and Swapan Chakrabarti*

Department of Chemistry, University of Calcutta, 92, A. P. C. Ray Road, Kolkata 700009, India

Received: October 22, 2008; Revised Manuscript Received: December 10, 2008

The present work aims to establish the suitability of double hybrid density functionals in explaining the potential energy curves of carbon dioxide−rare gas (CO_2-Rg; Rg: He, Ne, Ar, and Kr) systems. The interaction energies of the most stable T-shaped configuration of all CO_2-Rg systems have been evaluated using pure gradient-corrected functionals and double hybrid density functionals and their dispersion-corrected analogs with the use of Dunning's augmented correlation consistent polarized valence triple-ζ (aug-cc-pVTZ) basis function. The equilibrium separation distance, r, between CO_2 and Rg obtained from the potential energy curves for these CO_2-Rg systems are then compared with the experimental as well as with some earlier theoretical non-density functional theory (non-DFT) results. Our investigation suggests that for CO_2-Ar/Kr systems, the r values obtained using the short-range corrected double hybrid mPW2PLYP functional is in excellent agreement with the experimental distances of separation. On the other hand, the short-range corrected double hybrid B2PLYP functional reproduces the experimental r values for the CO_2-He/Ne systems quite satisfactorily. Interestingly, for lighter CO_2-Rg (Rg: He and Ne) complexes, the B2PLYP functional fails to explain the potential energy surface, whereas the mPW2PLYP functional satisfactorily explains the potential well depth. On the other hand, for higher Rg complexes, none of the functionals are able to produce satisfactory potential well depth. Hence, the overall investigation suggests that, although double hybrid density functionals and other density functionals are good for predicting separation distance, they fail to produce correct interaction energy values in higher CO_2-Rg complexes.

Introduction

The noncovalent interactions between atoms and molecules have versatile applications in various fields of chemistry. In the supramolecular architecture, such as host−guest interactions, bucky catchers, drug binding, and so forth, these interactions play a crucial role.[1−3] The role of these weak interactions in enzyme−substrate binding, intercalation of drugs in DNA,[4,5] and in interstellar chemistry is also of great significance. Of several weakly bound systems or van der Waals (vdW) complexes, carbon dioxide−rare gas (CO_2-Rg) is one of the simplest prototypes to understand the nature of intermolecular interactions between nonpolar units. CO_2, being an important absorber of infrared (IR) radiation in the Earth's atmosphere, the complexes formed by Rg and CO_2 also have an important role to play in the atmospheric and interstellar chemistry.[6−8]

Among all the CO_2-Rg systems studied so far, the argon (Ar) complex is the one mostly investigated.[9−13] Experimental results suggest a T-shaped geometry for this vdW system. The group of Steed, Dixon, and Klemperer[9] made a successful attempt in this direction, and confirmed the T-shaped equilibrium geometry of CO_2-Ar via radiofrequency and microwave spectroscopic methods. Later on, Fraser et al.[10,11] reported the subdoppler IR spectra and vibrational predissociation linewidths of some CO_2-Rg (Rg: neon (Ne), argon (Ar), and krypton (Kr)) systems using an optothermal molecular beam laser spectrometer. The IR spectra obtained for each of these systems are well in accordance with the T-shaped geometry proposed by Steed et al.[9] Sharpe and co-workers[14] studied the rovibrational spectrum of CO_2-Ar using a pulsed and tunable IR diode laser. In an elegant attempt, Weida et al.[15] for the first time characterize the CO_2−helium (He) complex based on high-resolution, direct absorption spectroscopic methods in the IR region of the spectrum. Recently, Vigasin et al.[16] tried to figure out the IR and Raman spectra of CO_2 monomers and dimers trapped in various matrices including an Rg matrix and tried to correlate the CO_2 frequency shifts with the critical temperature of the matrix material.

Apart from the spectroscopic analyses, there are numerous investigations based on the determination of the potential energy surface (PES) for different CO_2-Rg systems employing both ab initio techniques[7,17−20] as well as empirical methods.[21−26] The first realistic potential energy curve (PEC) for a CO_2-Rg (Rg: He) system was proposed by Parker et al.[21] They used the electron gas model and a vdW interaction term in order to account for the short- and long-range interactions, respectively. However, this PSP (Parker, Snow, and Pack) potential[21] has a very poor representation of the attractive well. Later, Stroud and Raff[18] obtained an attractive ab initio PES using the self-consistent field method. In another work, Marshall et al.,[20] for the first time, determined the PES of the CO_2-Ar complex using the first principles method. They used Møller−Plesset perturbation theory using supermolecular approach (S-MPPT) in order to construct the PES and also calculated several parameters of interest, including dispersion energies. Roche and co-workers[26] generated two new PESs for the CO_2-Ar system by least-squares fitting to the high-resolution microwave data. The

* Corresponding author. E-mail: swapanchem@yahoo.co.in. Fax: 91-33-23519755.

10.1021/jp809341g CCC: $40.75
Published on Web 01/15/2009

TABLE 1: Description of the Six Functionals (PBE, PBE+D, B2PLYP, B2PLYP+D, mPW2PLYP, and mPW2PLYP+D) used in the Present Study[a]

	density functionals					
	gradient corrected density functionals		double hybrid density functionals			
description	PBE	PBE+D	B2PLYP	B2PLYP+D	mPW2PLYP	mPW2PLYP+D
exchange functional	PBEx	PBEx	B88	B88	mPW	mPW
correlation functional	PBEc	PBEc	LYP	LYP	LYP	LYP
fraction of HF exchange (a_x)			0.53	0.53	0.55	0.55
fraction of GGA exchange (1-a_x)			0.47	0.47	0.45	0.45
fraction of LYP correlation (a_c)			0.73	0.73	0.75	0.75
Møller−Plesset type perturbative correction (1-a_c)			0.27	0.27	0.25	0.25
final C_6 coefficient scaling factor (s_6)		0.75		0.55		0.40

[a] The values for the parameters are taken from the ref 40.

resulting potential obtained by them quite satisfactorily explains the experimental results.

The problem of using highly correlated methods is that they are time-consuming and computationally very costly, and this can easily be removed if one uses density functional theory (DFT) and incorporates appropriate dispersion-corrected potentials in it.[27,28] In this context, it should be noted that, over a period of time, several new functionals have also been designed that give good results for various kinds of intermolecular interactions.[29] Recently, Grimme[30,31] started using dispersion-corrected density functional theory (DFT-D) which is an enhancement of similar methods developed earlier.[32] The dispersion correction in this method is described by damped interatomic R^{-6} potentials. Grimme furthermore showed that, by using the DFT-D method and triple-ζ quality basis sets, much of the laborious basis set superposition error (BSSE)[33] is avoided, which is otherwise very essential in the case of highly correlated methods.[34]

In an earlier work, Zhao et al.[35] developed a new approach of combining nonlocal exchange with the local one in the density functional (first hybrid), and then the density functional is combined with a wave function correlation expression (second hybrid). The approach developed was called double hybrid density functional (DHDF) theory. Since then, several DHDFs have been developed[36−39] are are found to be very effective in explaining different physicochemical properties. These include thermochemistry and thermochemical kinetics of main group elements, pericyclic reactions, higher transition metal reactions, and so forth. Recently, Grimme and co-workers[36,37] developed two new DHDFs, namely, B2PLYP and mPW2PLYP. They also incorporate dispersion correction to the above-mentioned DHDFs, which is capable of treating long-range as well as medium-range dispersion effects.[40] In the present investigation, we intend to see whether the newly developed B2PLYP and mPW2PLYP DHDFs and their dispersion-corrected counterparts are suitable in explaining the PECs of four CO_2−Rg (Rg: He, Ne, Ar, and Kr) systems.

Computational Details

The PECs for all the CO_2−Rg systems that are studied here are constructed employing six density functional methods. Two of them, i.e., Perdew−Burke−Ernzerhof (PBE)[41] and PBE+D, are the gradient corrected functionals, while the other four (B2PLYP, B2PLYP+D, mPW2PLYP, and mPW2PLYP+D) are their double hybrid counterparts as mentioned earlier. The extension "+D" stands for the long-range dispersion-corrected functionals containing the interaction term. In this section, we provide a detailed description of these six functionals that are used in the present investigation.

As mentioned earlier, the newly developed DHDFs proposed by Grimme and co-workers in 2006 (B2PLYP[36] and mPW2PLYP[37]) are based on the mixing of standard generalized gradient approximation (GGA) functionals with Hartree−Fock (HF) exchange and a Møller−Plesset type perturbation correction of second order, which originates from the Kohn−Sham (KS) orbitals and eigenvalues. In B2PLYP,[36] Becke 88 (B88) exchange and Lee−Yang−Parr (LYP) correlation was implemented, whereas in the mPW2PLYP functional,[37] only the exchange term is replaced by the modified Perdew−Wang (mPW) functional of Adamo and Barone.[42] In this context, it is wise to mention that some of the popular functionals such as M05-2X, M06-L, and M06-2X also account well for dispersion-like interactions at medium range.[43]

The DHDF energy can therefore be written as the combination of the hybrid functional and the second order perturbative correction term as follows:

$$E_{\mathrm{DHDF}} = E_{\mathrm{XC}}^{\text{Hybrid-GGA}} + (1 - a_c)E_{\mathrm{C}}^{\text{KS-PT2}} \quad (1)$$

where the first term corresponds to a standard hybrid density functional, and the second one corresponds to the Møller−Plesset type perturbative correction term with the coefficient $(1 - a_c)$.[37] The second term in eq 1 is simply a postulated addition to the KS energy. The two terms on the right-hand side of the above equation can explicitly be written by the following expressions:[36,37]

$$E_{\mathrm{XC}}^{\text{Hybrid-GGA}} = (1 - a_x)E_{\mathrm{X}}^{\mathrm{GGA}} + a_x E_{\mathrm{X}}^{\mathrm{HF}} + a_c E_{\mathrm{C}}^{\mathrm{GGA}} \quad (2)$$

and

$$E_{\mathrm{C}}^{\text{KS-PT2}} = \frac{1}{4}\sum_{ia}\sum_{jb}\frac{|\langle ij||ab\rangle|^2}{\varepsilon_i + \varepsilon_j - \varepsilon_a - \varepsilon_b} \quad (3)$$

In eq 2, a_x and a_c are fractions of the HF exchange and the GGA correlation (here it is LYP correlation), respectively. These two parameters are the global scaling factors and have been determined empirically by Grimme and co-workers for B2PLYP and mPW2PLYP DHDFs.[36,37] The values for the relevant parameters are depicted in Table 1. In eq 3, the Møller−Plesset type perturbative correction term contains the occupied KS orbitals labeled as i and j, while the labels a and b are for the virtual ones. The one-particle energies are given by ε containing terms in the denominator.

Although the DHDFs give satisfactory results (minimum error) compared to that of other hybrid and GGA functionals, particularly for larger and complicated molecular systems, still it lacks the description of dispersion forces.[40] Earlier, dispersion correction to the mean field level of theory (HF, DFT) was introduced by several groups.[32,44] In 2004 and also in 2006, Grimme adopted the same methodology (to GGA functionals)

where a pairwise additive potential of the form C_6R^{-6} is applied to account for the long-range dispersion effects.[30,31] The total density functional energy (including DHDF) can then be written as follows:

$$E_{\text{DFT-D}} = E_{\text{KS-DFT}} + E_{\text{vdW}} \quad (4)$$

where $E_{\text{KS-DFT}}$ is the normal self-consistent density functional energy, and E_{vdW} is an empirical dispersion correction term, which is given by

$$E_{\text{vdW}} = -s_6 \sum_{i=1}^{N-1} \sum_{j=i+1}^{N} \frac{C_6^{ij}}{R_{ij}^6} f_{\text{dmp}}(R_{ij}) \quad (5)$$

Here s_6 is a scaling factor that depends exclusively on the density functional/semiempirical method used, C_6^{ij} is the combined dispersion coefficient for the pair of atoms i and j, R_{ij} is the interatomic distance between atoms i and j, $f_{\text{dmp}}(R_{ij})$ is the damping function, and N is the number of atoms in the system. The mathematical expression of the damping function, $f_{\text{dmp}}(R_{ij})$ chosen here is

$$f_{\text{dmp}}(R_{ij}) = \frac{1}{1 + e^{-d(R/R_0 - 1)}} \quad (6)$$

where d is taken to be 20 in the exponent, and it gives larger corrections at intermediate distances.[31] There are several mathematical expressions for the dispersion coefficient C_6^{ij}, but the one that produced better results for elements up to xenon is taken here. This expression is the geometric mean of individual atomic C_6 coefficients,[31] i.e.,

$$C_6^{ij} = \sqrt{C_6^i C_6^j} \quad (7)$$

As the scaling factor s_6 depends exclusively on the functionals used, it should be different for different density functionals. For the gradient-corrected PBE functional, Grimme determined the s_6 factor by least-squares optimization of the deviations observed in the interaction energy values for various weakly interacting systems.[31] On the other hand, for the DHDFs, the s_6 factor is determined from the variation of the mean absolute deviation (MAD) of both the B2PLYP and mPW2PLYP functionals at different values of the scaling factor.[40] The relevant s_6 values are given in Table 1 for the dispersion-corrected density functionals.

As mentioned earlier, the PECs have been obtained using PBE, B2PLYP, and mPW2PLYP (both with and without dispersion correction) functionals along with Dunning's augmented correlation consistent polarized valence triple-ζ (aug-cc-pVTZ) basis.[45] The DHDFs and dispersion-corrected functionals are well implemented in the ORCA[46] suite of programs. The Rg atom is placed perpendicular to the molecular axis of CO_2, i.e., a perfect T-shaped geometry. The scanning of the interaction energies is then performed by varying the distance of separation, r, between CO_2 and Rg and calculating the single point energies at each r value without disturbing the perfect T-shaped geometry of the complexes. It is to be noted that r is the center-to-center distance between the carbon atom of the CO_2 molecule and the Rg atom.

Results and Discussion

A schematic representation of the CO_2−Rg systems is depicted in Figure 1 along with the separation parameter, r. The CO_2 molecule is linear, with the C═O bond length being 1.163 Å.[9] There can be two possible conformers for the CO_2−Rg complexes. One is the T-shaped geometry, which has been discussed in the previous section, while the other one is the linear structure with the Rg atom placed at one end of the CO_2 moiety, near one of the oxygen atoms in the same plane. Earlier, potential energy results confirmed the presence of both these conformers,[6,7] with the T-shaped geometry residing in the energy valley (global minimum energy value) and the linear one with slightly more energy than the former. It is to be noted that, in the present investigation, we have taken the perfect T-shaped geometry for each of these systems, which will be much more clear by looking at Figure 1.

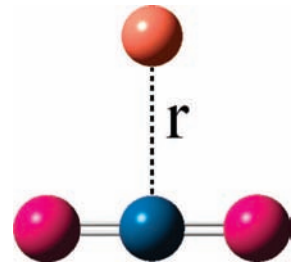

Figure 1. A schematic representation of the T-shaped structures of CO_2−Rg (Rg: He, Ne, Ar, and Kr) systems. The blue ball represents the carbon atom, the pink ones are the oxygen atoms, and the orange represents the Rg atoms.

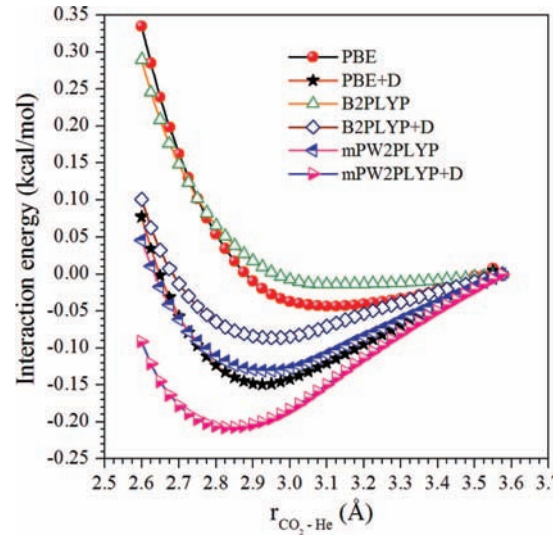

Figure 2. Comparison of the PECs for the T-shaped CO_2−He system using gradient-corrected PBE density functional and double-hybrid B2PLYP and mPW2PLYP density functionals (both with and without dispersion corrections). Here, r_{CO_2-He} is the center-to-center distance of separation between the carbon atom of the CO_2 molecule and He. The distance is varied as shown in Figure 1.

Before going into the discussion of the PECs for each of these systems, we would like to mention three important points. The first one is that the experimental geometries for CO_2−Rg systems are not a perfect T-shaped structure, but have a slightly bent T-like geometry. The second point is that we have not considered the CO_2−xenon (Xe) system in this work. This is because Xe, being a heavy element, is highly influenced by the relativistic effect, and the properties of the systems containing Xe atom(s) are strongly affected as a result of this effect compared to the geometries without Xe atom(s).[47] On the other hand, the effect of relativity is not so pronounced for rare gases up to Kr.[47,48] The third one is that, in all the PEC scans, the interaction energies are calibrated with respect to the energy value at highest separation distance for each of the CO_2−Rg systems studied.

TABLE 2: The Equilibrium Distance Obtained from the PES Scanning for Different CO_2−Rg (Rg: He, Ne, Ar, and Kr) Systems Using Different Methodologies[a]

systems	distance of separation between CO_2 and Rg corresponding to the minimum energy value obtained from the PEC scan (Å)							
	PBE	PBE+D	B2PLYP	B2PLYP+D	mPW2PLYP	mPW2PLYP+D	earlier theoretical non-DFT results	experimental results
CO_2−He	3.125	2.925	3.125	2.950	2.950	2.825	3.100[b] 3.078[c] 3.070[d]	3.581[j]
CO_2−Ne	3.350	3.050	3.275	3.000	3.025	2.950	3.200[b]	3.2904[k]
CO_2−Ar	3.775	3.450	3.625	3.400	3.500	3.375	3.475[e]3.416[f] 3.417[g] 3.418[h] 3.459[i]	3.493[l]
CO_2−Kr	3.925	3.575	3.725	3.525	3.625	3.500		3.6249[m]

[a] The basis set used is Aug-cc-pVTZ. Some of the previous theoretical results and experimental distances of separation are also given for comparison. [b] Reference 7: MP4 with cc-pVTZ (C and O) and aug- cc-pVTZ (He), 6-311+G(3d,2f) (Ne). [c] Reference 49: symmetry-adapted perturbation theory (SAPT). [d] Reference 49: CCSD(T) result. [e] Reference 20: S-MPPT result. [f] Reference 26: single repulsion. [g] Reference 26: split repulsion. [h] Reference 55: SAPT result. [i] Reference 55: CCSD(T) result using supermolecular approach. [j] Reference 15. [k] Reference 51. [l] Reference 9. [m] Reference 10.

TABLE 3: Magnitude of the Interaction Energies Corresponding to the Equilibrium Distance Obtained from the PES Scanning for Different CO_2−Rg (Rg: He, Ne, Ar, and Kr) Systems Using Different Methodologies[a]

systems	magnitude of the interaction energies of the potential well depth of the CO_2−Rg (Rg: He, Ne, Ar and Kr) obtained from the PEC scan (kcal)						
	PBE	PBE+D	B2PLYP	B2PLYP+D	mPW2PLYP	mPW2PLYP+D	earlier theoretical non-DFT results
CO_2−He	0.043	0.149	0.014	0.086	0.131	0.207	0.131[b] 0.144[c] 0.141[d]
CO_2−Ne	0.046	0.224	0.054	0.222	0.197	0.360	0.242[b]
CO_2−Ar	0.027	0.275	0.073	0.288	0.195	0.383	0.600[e] 0.584[f] 0.579[g] 0.633[h] 0.560[i]
CO_2−Kr	0.038	0.354	0.101	0.387	0.217	0.452	

[a] The basis set used is Aug-cc-pVTZ. Some of the previous theoretical results are given for comparison. [b] Reference 7: MP4 with cc-pVTZ (C and O) and aug- cc-pVTZ (He), 6-311+G(3d,2f) (Ne). [c] Reference 49: SAPT result. [d] Reference 49: CCSD(T) result. [e] Reference 20: S-MPPT result. [f] Reference 26: single repulsion. [g] Reference 26: split repulsion. [h] Reference 55: SAPT result. [i] Reference 55: CCSD(T) result using supermolecular approach.

Among the four CO_2−Rg systems that are studied in the present investigation, CO_2−He and CO_2−Ar are the ones widely investigated. The CO_2−He system is of great significance as it provides necessary information on the trends observed in different intermolecular properties on changing the polarizability of Rg.[6] There has been a lot of investigation to calculate the intermolecular PES of this system using both ab initio techniques[7,17−19] and empirical methods.[21−25] In the present work, we compare our results obtained from the PECs of the CO_2−He system with the experimental findings of Weida et al.[15] and also with some of the previous theoretical non-DFT results, including that of coupled cluster (CCSD(T)) results.[49] Figure 2 presents the variation of the interaction energies with the separation distance, r, for CO_2−He using different methods. In each case, a distinct minimum is observed; however, for PBE and B2PLYP, the minimum observed is very shallow in nature. In order to compare our results with the experimental as well as with the non-DFT results, we provide Table 2, where the equilibrium r values corresponding to minimum energy obtained from the PECs is given for each system studied. From the table, it is quite clear that neither the DHDFs nor the PBE functional corroborate with the experimental separation distance. The r values obtained using PBE and short-range corrected B2PLYP methods are 0.46 Å shorter than the experimental value, whereas the long-range dispersion-corrected functionals underestimate the distance by an amount of 0.65 to 0.75 Å. If one compares the equilibrium distance obtained with more accurate and sophisticated CCSD(T) results, he will find a close agreement of the CCSD(T) distance with B2PLYP and PBE results. On the contrary, all the other DHDFs and dispersion-corrected density functionals fail to produce the CCSD(T) results. The interaction energies corresponding to the potential well depth have also been tabulated in Table 3 along with those obtained in the present study. A close inspection of Table 2 and Table 3 reveals an interesting observation. The mPW2PLYP and PBE+D functionals quite satisfactorily produce the interaction energies and are well in agreement with the earlier results including CCSD(T), but the separation distance obtained with these two functionals (Table 2) are far from the non-DFT results. On the other hand, the distances obtained using B2PLYP and PBE functionals match well with the non-DFT results, but the interaction energies of the potential well depth are nowhere near those earlier theoretical non-DFT results.

The second system that has been investigated here is CO_2−Ne. Although there have been a lot of investigations on the He complex, only limited research work has been performed on the CO_2−Ne[7,10,11,16] complex. As previously mentioned, it has got a T-shaped geometry, which is also consistent with the

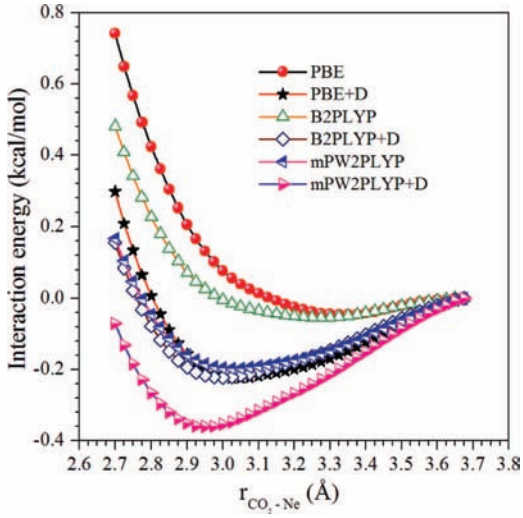

Figure 3. Comparison in the PECs for the T-shaped CO_2−Ne system using gradient-corrected PBE density functional and double-hybrid B2PLYP and mPW2PLYP density functionals (both with and without dispersion corrections). Here, r_{CO_2-Ne} is the center-to-center distance of separation between the carbon atom of the CO_2 molecule and Ne. The distance is varied as shown in Figure 1.

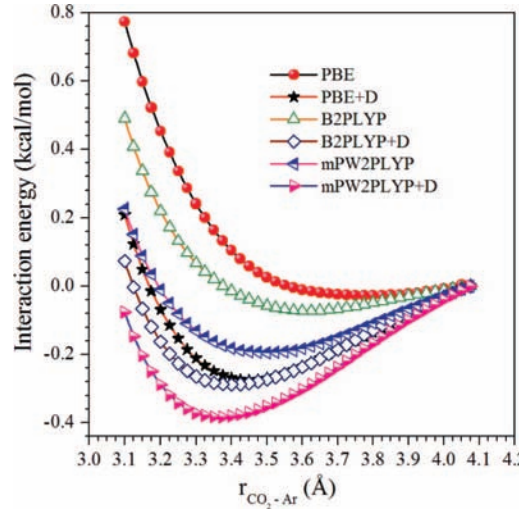

Figure 4. Comparison in the PECs for the T-shaped CO_2−Ar system using gradient-corrected PBE density functional and double-hybrid B2PLYP and mPW2PLYP density functionals (both with and without dispersion corrections). Here r_{CO_2-Ar} is the center-to-center distance of separation between the carbon atom of the CO_2 molecule and Ar. The distance is varied as shown in Figure 1.

spectroscopic analyses.[10,11] Endo and co-workers[50] studied the rotational spectra of various CO_2−Rg complexes, including that of CO_2−Ne through the Fourier-transform microwave spectroscopic method. The first ab initio PES study for CO_2−Ne was carried out by Negri et al.[7] using the MP4 method along with Dunning's augmented basis and Pople's diffusion and polarization containing basis sets. In the present work, we have also used Dunning's aug-cc-pVTZ basis set for the PES scanning. The relevant scanning curve for CO_2−Ne is plotted against the distance of separation, r, in Figure 3. Just like CO_2−He, a distinct minimum in the PEC scan is observed at each level of theory except that at PBE and B2PLYP, where the minima obtained are shallow in nature. It is quite evident from Table 2 that the short-range corrected B2PLYP functional satisfactorily produces the experimental CO_2−Ne separation distance[51] with an error of only 0.02 Å. It also matches well with the MP4 results of Negri et al.[7] However, the interaction energy obtained using this B2PLYP functional (Table 3) is very far from the non-DFT results of Negri et al.[7] On the other hand, the mPW2PLYP and all the long-range corrected dispersion-corrected functionals underestimate the r values by 0.2−0.35 Å, but the interaction energies of the potential well depth obtained from the dispersion-corrected B2PLYP and PBE functionals along with the mPW2PLYP (DHDF) functional are in accordance with that of Negri et al.[7] Similar observations are also found in the case of the CO_2−He complex.

The CO_2−Ar system is considered as one of the simplest prototypes to understand the interactions of an atom with a linear triatomic molecule.[52] The first successful attempt in characterizing this system was done by the group of Steed, Dixon, and Klemperer,[9] who also confirmed the T-shaped geometry of CO_2−Ar by molecular beam electronic resonance spectroscopy. Since then, a lot of work has been done in order to get reliable PES, which can reproduce the spectra of this vdW complex and also the pressure broadening of CO_2 IR lines by Ar. The CO_2−Ar system has also been investigated using IR spectroscopic techniques.[14,53] Roche et al.[54] tested the ability of nine different PESs to reproduce the experimental results. The results obtained by them suggest that all those potentials give significant discrepancies in at least one of the spectroscopic properties, and it was concluded that a new PES should be constructed to resolve those discrepancies. In another work, Horst and Jameson[52] compared the ability of 12 PESs that have then been proposed for the CO_2−Ar system in explaining different physicochemical properties. Misquitta et al.[55] calculated the PES for the CO_2−Ar complex at different levels of theory such as symmetry-adapted perturbation theory (SAPT), many-body perturbation theory (MBPT), and coupled cluster methods, both using supermolecular approach, in order to determine the rovibrational spectra of this complex and the virial coefficients. The interaction energies that are calculated in the present investigation for CO_2−Ar is plotted against r and is depicted in Figure 4. Like the other two systems, here also the scan shape reveals distinct minima in all the methods used, except while using the PBE functional, where the same is very shallow. An inspection of the relevant data for CO_2−Ar given in Table 2 clearly reflects the role of short-range corrected mPW2PLYP functional on stabilizing this complex. As mentioned by Grimme in his paper revealing the mPW2PLYP functional gives the lowest MAD and is very effective for weak interactions,[37] its nature is reflected in the equilibrium separation distance obtained (3.500 Å), which is in excellent agreement with the experiment (3.493 Å).[9] The MBPT results using supermolecular approach[20] are also quite close to those of our mPW2PLYP and the experimental results. However, the distances obtained from all the density functionals adopted do not match with the highly sophisticated CCSD(T) level of theory, except that obtained from dispersion-corrected PBE functional. The normal PBE functional overestimates the separation distance by 0.28 Å, while its long-range dispersion-corrected analogue is close to the experimental results with a difference of 0.04 Å. Similar is the situation for the B2PLYP functional, which overestimates the r value by an amount of 0.13 Å. The dispersion-corrected counterpart of B2PLYP is consistent with the earlier theoretical results of Hutson et al.[26] and the SAPT result of Misquitta et al.[55] At this point it is highly instructive to mention that, as the experimental geometry of CO_2−Ar complex is not a perfect T shape but has a bent T-like geometry, we have also carried out a PEC scanning on this bent geometry, and the relevant PES is given in the Supporting Information. From the PEC scanning, it is clear that the location and depth of the global minimum is only slightly

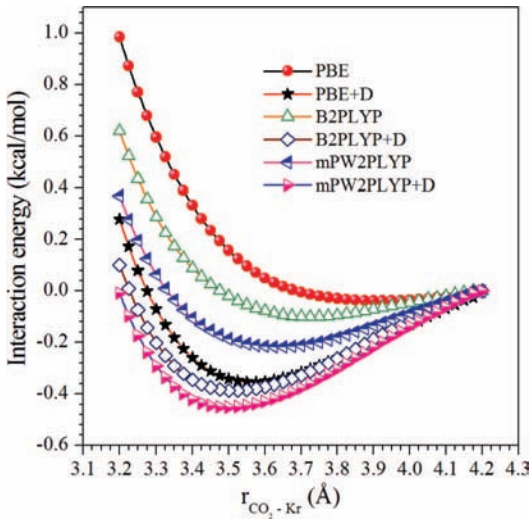

Figure 5. Comparison of the PECs for the T-shaped CO_2-Kr system using gradient-corrected PBE density functional and double-hybrid B2PLYP and mPW2PLYP density functionals (both with and without dispersion corrections). Here r_{CO_2-Kr} is the center-to-center distance of separation between the carbon atom of the CO_2 molecule and Kr. The distance is varied as shown in Figure 1.

affected in bent geometry relative to that of the perfect T-shaped geometry. In Table 3, the interaction energy values for the CO_2-Ar complex are tabulated, and some very interesting results are observed. Although it has been observed that, for lighter CO_2-Rg (Rg: He and Ne) complexes, at least some of the density functionals satisfactorily reproduce the interaction energies and corroborate with the non-DFT results; however, for the CO_2-Ar complex, none of the interaction energy values obtained in the present study match with that of the earlier non-DFT results, which include CCSD(T) calculations as well. The magnitude for the highest interaction energy is 0.383 kcal (mPW2PLYP+D functional), which is underestimated by an amount of 0.20−0.25 kcal relative to the previous results.

The last system that we have chosen in this work is the CO_2-Kr complex. To date, very few investigations have been performed related to the stability of this system.[10,16,50] Fraser, Pine, and Suenram[10] reported the IR spectra of several CO_2-Rg systems, including that of CO_2-Kr, using a molecular beam laser spectrometer. The weak bond stretching force constant in the CO_2-Kr complex was found to be quite large compare to that of CO_2-Ar. Hence, the dispersion forces will definitely play a dominant role and will be much more pronounced in the Kr complex relative to the Ar analogue. Pure rotational spectra of this system were also studied. Iida et al.[50] proposed a model calculation that describes intermolecular potential in CO_2-Rg systems. The observed transitions reported in their work[50] were also consistent with the T-shaped geometry of this system. In the present study, Figure 5 presents the PEC scans of the CO_2-Kr system. Similar to the Ar complex, a distinct minimum is observed in each of the methods implemented, with the only exception at PBE, where the minimum is pretty shallow in nature. Table 2 reveals that the separation distances obtained using long-range dispersion-corrected functionals are within the range of 0.1 Å, whereas the normal PBE and B2PLYP functionals have their r values overestimated by 0.3 and 0.1 Å, respectively. Most impressive is the result observed using the short-range mPW2PLYP functional, where the equilibrium r value obtained from the present PEC scan is only 0.0001 Å larger than the experimental value.[10] The interaction energies corresponding to the potential well depth for the CO_2-Kr complex is given in Table 3. To the best of our knowledge, there has been no theoretical investigation on this Kr complex relative to the PES. Hence, we are unable to provide any other data of interaction energies for the CO_2-Kr complex.

In the present investigation, the effect of basis set has also been explored. Very recently, Martin and co-workers[38,39] provide a detailed discussion on the basis set sensitivity in various double hybrid functionals. In order to see the basis set sensitivity, the PEC scanning for all CO_2-Rg systems are performed using the B2PLYP functional along with the use of Dunning's augmented triple and double-ζ polarized basis sets. The relevant scanning curves given in the Supporting Information (Figures F2−F5) clearly indicate that the basis sets have little effect in influencing the PECs of CO_2-Rg systems, with the only exception observed for the CO_2-Ar complex.

Conclusions

In the present study, we investigate whether the DHDFs and other density functionals are suitable in explaining the PECs of four CO_2-Rg (Rg: He, Ne, Ar, and Kr) systems. The results are also compared with the experimental and some earlier theoretical non-DFT values. Most impressive are the results obtained for CO_2-Ar/Kr systems, where the short-range corrected double hybrid mPW2PLYP functional remarkably reproduces the experimental distance of separation between CO_2 and Rg atoms in these weakly bound complexes with errors as low as 0.2% and 0.003%, respectively. On the other hand, for the CO_2-He/Ne complexes, the r values obtained by the short-range corrected double hybrid B2PLYP functional is consistent with the experiment. The long-range dispersion-corrected functionals fail to reproduce the experimental data for the CO_2-Rg systems. Another interesting observation is that, for the lighter CO_2-Rg (Rg: He and Ne) complexes, B2PLYP functional fails to produce the correct interaction energies of the potential well depth, whereas the mPW2PLYP functional quite satisfactorily produces the interaction energies and explains the PES. Moreover, it has also been observed that change in the angle between CO_2 and Rg does not change the nature of the PECs. The overall investigation, hence, suggests that, although these DHDFs and other density functionals are good to predict the separation distance, they failed to produce correct interaction energy values in higher CO_2-Rg complexes. To explicate the role of different basis sets and other DHDFs in explaining the PECs of CO_2-Rg systems, a detailed analysis will be performed in the near future.

Acknowledgment. P.S. would like to thank UGC, Govt. of India, for his fellowship. S.C. acknowledges the financial support (UPE Project) for providing us 8 CPU cluster machine. The authors also wish to convey their special thanks to Prof. W. Klemperer and his groups for providing us with important references on the experimental results for the CO_2-Rg systems.

Supporting Information Available: A comparison of the PECs for the CO_2-Ar complex between the perfect T-shaped geometry and the bent T-shaped geometry performed at the mPW2PLYP/Aug-cc-pVTZ level of theory, and comparisons of the PECs for all CO_2-Rg complexes studied at the B2PLYP level of theory using the Aug-cc-pVTZ and Aug-cc-pVDZ basis sets (basis set sensitivity). This material is available free of charge via the Internet at http://pubs.acs.org.

References and Notes

(1) *Supramolecular Chemistry: Concepts and Perspectives*; Lehn, J.-M., Ed.; VCH: NewYork, 1995.

(2) Steed, J. W.; Atwood, J. L. *Supramolecular Chemistry: A Concise Introduction*; Wiley: New York, 2000.
(3) (a) Hunter, C. A. *Chem. Soc. Rev.* **1994**, *23*, 101. (b) Sygula, A.; Fronczek, F. R.; Sygula, R.; Rabideau, P. W.; Olmstead, M. M. *J. Am. Chem. Soc.* **2007**, *129*, 3842.
(4) (a) Zimm, B. H. *J. Chem. Phys.* **1960**, *33*, 1349. (b) Burley, S. K.; Petsko, G. A. *Science* **1985**, *229*, 23. (c) Hunter, C. A.; Singh, J.; Thornton, J. M. *J. Mol. Biol.* **1991**, *218*, 837.
(5) *Principles of Nucleic Acid Structure*; Saenger, W., Ed.; Springer-Verlag: New York, 1984.
(6) Yan, G.; Yang, M.; Xie, D. *J. Chem. Phys.* **1998**, *109*, 10284.
(7) Negri, F.; Ancilotto, F.; Mistura, G.; Toigo, F. *J. Chem. Phys.* **1999**, *111*, 6439.
(8) Roche, C. F.; Ernesti, A.; Hutson, J. M.; Dickinson, A. S. *J. Chem. Phys.* **1996**, *104*, 2156.
(9) Steed, J. M.; Dixon, T. A.; Klemperer, W. *J. Chem. Phys.* **1979**, *70*, 4095.
(10) Fraser, G. T.; Pine, A. S.; Suenram, R. D. *J. Chem. Phys.* **1988**, *88*, 6157.
(11) Pine, A. S.; Fraser, G. T. *J. Chem. Phys.* **1988**, *89*, 100.
(12) Severson, M. W. *J. Chem. Phys.* **1998**, *109*, 1343.
(13) Jovan Jose, K. V.; Gadre, S. R. *J. Chem. Phys.* **2008**, *128*, 124310.
(14) Sharpe, S. W.; Reifschneider, D.; Wittig, C.; Beaudet, R. A. *J. Chem. Phys.* **1991**, *94*, 233.
(15) Weida, M. J.; Sperhac, J. M.; Nesbitt, D. J.; Hutson, J. M. *J. Chem. Phys.* **1994**, *101*, 8351.
(16) Vigasin, A. A.; Schriver-Mazzuoli, L.; Schriver, A. *J. Phys. Chem. A* **2004**, *104*, 5451.
(17) (a) Pack, R. T. *J. Chem. Phys.* **1974**, *61*, 2091. (b) Pack, R. T. *J. Chem. Phys.* **1976**, *64*, 1659.
(18) Stroud, C. L.; Raff, L. M. *J. Chem. Phys.* **1980**, *72*, 5479.
(19) Keil, M.; Rawluik, L. J.; Dingle, T. W. *J. Chem. Phys.* **1992**, *96*, 6621.
(20) Marshall, P. J.; Szczêśniak, M. M.; Sadlej, J.; Chałasiński, G.; Ter Horst, M. A.; Jameson, C. J. *J. Chem. Phys.* **1996**, *104*, 6569.
(21) Parker, G. A.; Snow, R. L.; Pack, R. T. *J. Chem. Phys.* **1976**, *64*, 1668.
(22) Keil, M.; Parker, G. A.; Kupperman, A. *Chem. Phys. Lett.* **1978**, *59*, 443.
(23) Parker, G. A.; Keil, M.; Kupperman, A. *J. Chem. Phys.* **1983**, *78*, 1135.
(24) Keil, M.; Parker, G. A. *J. Chem. Phys.* **1985**, *82*, 1947.
(25) Beneventi, L.; Casavecchia, P.; Vecchiocattivi, F.; Volpi, G. G.; Buck, U.; Lauenstein, C.; Schinke, R *J. Chem. Phys.* **1988**, *89*, 4671.
(26) Hutson, J. M.; Ernesti, A.; Law, M. M.; Roche, C. F.; Wheatley, R. J. *J. Chem. Phys.* **1996**, *105*, 9130.
(27) Kamiya, M.; Tsuneda, T.; Hirao, K. *J. Chem. Phys.* **2002**, *117*, 6010.
(28) Jha, P. C.; Rinkevicius, Z. R.; Ågren, H.; Seal, P.; Chakrabarti, S. *Phys. Chem. Chem. Phys.* **2008**, *10*, 2715.
(29) (a) Zhao, Y.; Truhlar, D. G. *Phys. Chem. Chem. Phys.* **2005**, *7*, 2701. (b) Zhao, Y.; Schultz, N. E.; Truhlar, D. G. *J. Chem. Theory. Comput.* **2006**, *2*, 364. (c) Puzder, A.; Dion, M.; Langreth, D. C. *J. Chem. Phys.* **2006**, *124*, 164105. (d) Becke, A. D.; Johnson, E. R. *J. Chem. Phys.* **2005**, *123*, 154105. (e) Zhao, Y.; Truhlar, D. G *J. Phys. Chem. A* **2005**, *109*, 4209.
(30) Grimme, S. *J. Comput. Chem.* **2004**, *25*, 1463.
(31) Grimme, S. *J. Comput. Chem.* **2006**, *27*, 1787.
(32) (a) Ahlrichs, R.; Penco, R.; Scoles, G *Chem. Phys.* **1977**, *19*, 119. (b) Elstner, M.; Hobza, P.; Frauenheim, T.; Suhai, S.; Kaxiras, E *J. Chem. Phys.* **2001**, *114*, 5149. (c) Wu, X.; Vargas, M. C.; Nayak, S.; Lotrich, V.; Scoles, G. *J. Chem. Phys.* **2001**, *115*, 8748. (d) Wu, Q.; Yang, W. *J. Chem. Phys.* **2002**, *116*, 515.
(33) Boys, S. F.; Bernardi, F. *Mol. Phys.* **1970**, *19*, 553.
(34) Parac, M.; Etinski, M.; Peric, M.; Grimme, S. *J. Chem. Theory Comput.* **2005**, *1*, 1110.
(35) Zhao, Y.; Lynch, B. J.; Truhlar, D. G. *J. Phys. Chem. A* **2004**, *108*, 4786.
(36) Grimme, S. *J. Chem. Phys.* **2006**, *124*, 034108.
(37) Schwabe, T.; Grimme, S. *Phys. Chem. Chem. Phys.* **2006**, *8*, 4398.
(38) Tarnopolsky, A.; Karton, A.; Sertchook, R.; Vuzman, D.; Martin, J. M. L. *J. Phys.Chem. A* **2008**, *112*, 3.
(39) Karton, A.; Tarnopolsky, A.; Lamère, J. F.; Schatz, G. C.; Martin, J. M. L. *J. Phys.Chem. A* **2008**, *112*, 12868.
(40) Schwabe, T.; Grimme, S. *Phys. Chem. Chem. Phys.* **2007**, *9*, 3397.
(41) Perdew, J. P.; Burke, K.; Ernzerhof, M. *Phys. Rev. Lett.* **1996**, *77*, 3865.
(42) Adamo, C.; Barone, V. *J. Chem. Phys.* **1998**, *108*, 644.
(43) (a) Zhao, Y.; Schultz, N. E.; Truhlar, D. G *J. Chem. Theory Comput.* **2006**, *2*, 364. (b) Zhao, Y.; Truhlar, D. G. *J. Chem. Phys.* **2006**, *125*, 194101.
(44) (a) Tang, K. T.; Toennies, J. P *J. Chem. Phys.* **1977**, *66*, 1496. (b) Tang, K. T.; Toennies, J. P. *J. Chem. Phys.* **1984**, *80*, 3726. (c) Douketis, C.; Scoles, G.; Marchetti, S.; Zen, M.; Thakkar, A. J. *J. Chem. Phys.* **1982**, *76*, 3057. (d) Merecero, J. M.; Maxtrain, J. M.; Lopez, X.; York, D. M.; Largo, A.; Eriksson, L. A.; Ugalde, J. M. *Int. J. Mass Spectrom.* **2005**, *240*, 37. and references therein. (e) Zimmerli, U.; Parrinello, M.; Koumoutsakos, P. *J. Chem. Phys.* **2004**, *120*, 2693.
(45) Woon, D. E.; Dunning, T. H., Jr *J. Chem. Phys.* **1993**, *98*, 1358.
(46) Neese, F. *ORCA−An Ab Initio, Density Functional and Semiempirical Program Package*, Version 2.6, revision 04 (2007); Institut fuer Physikalische und Theoretische Chemie, Universitaet Bonn: Germany, 2006 (p 45 of the ORCA manual).
(47) Radzio, E.; Andzelm, J. *J. Comput. Chem.* **1987**, *8*, 117.
(48) Faas, S.; Van Lenthe, J. H.; Snijders, J. G. *Mol. Phys.* **2000**, *98*, 1467.
(49) Korona, T.; Moszynski, R.; Thibault, F.; Launay, J.-M.; Bussery-Honvault, B.; Boissoles, J.; Wormer, P. E. S. *J. Chem. Phys.* **2001**, *115*, 3074.
(50) Iida, M.; Ohshima, Y.; Endo, Y. *J. Phys. Chem.* **1993**, *97*, 357.
(51) Randall, R. W.; Walsh, M. A.; Howard, B. J. *Faraday Discuss. Chem. Soc.* **1988**, *85*, 13.
(52) Ter Horst, M. A.; Jameson, C. J. *J. Chem. Phys.* **1996**, *105*, 6787.
(53) (a) Bohac, E. J.; Marshall, M. D.; Miller, R. E *J. Chem. Phys.* **1992**, *97*, 4890. (b) Bohac, E. J.; Marshall, M. D.; Miller, R. E *J. Chem. Phys.* **1992**, *97*, 4901.
(54) Roche, C. F.; Ernesti, A.; Hutson, J. M.; Dickinson, A. S. *J. Chem. Phys.* **1996**, *104*, 2156.
(55) Misquitta, A. J.; Bukowski, R.; Szalewicz, K. *J. Chem. Phys.* **2000**, *112*, 5308.

JP809341G